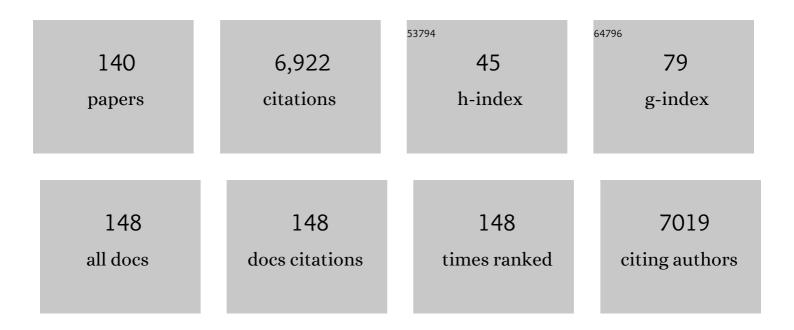
Simon R Bare

List of Publications by Year in descending order

Source: https://exaly.com/author-pdf/4756676/publications.pdf Version: 2024-02-01



#	Article	IF	CITATIONS
1	Structural evolution of atomically dispersed Pt catalysts dictates reactivity. Nature Materials, 2019, 18, 746-751.	27.5	404
2	Surface Structures of Supported Molybdenum Oxide Catalysts: Characterization by Raman and Mo L3-Edge XANES. The Journal of Physical Chemistry, 1995, 99, 10897-10910.	2.9	358
3	In Situ Spectroscopic Investigation of Molecular Structures of Highly Dispersed Vanadium Oxide on Silica under Various Conditions. Journal of Physical Chemistry B, 1998, 102, 10842-10852.	2.6	338
4	Morphology-dependent zeolite intergrowth structures leading to distinct internal and outer-surface molecular diffusion barriers. Nature Materials, 2009, 8, 959-965.	27.5	251
5	Identification of the active complex for CO oxidation over single-atom Ir-on-MgAl2O4 catalysts. Nature Catalysis, 2019, 2, 149-156.	34.4	222
6	Low-Temperature Restructuring of CeO ₂ -Supported Ru Nanoparticles Determines Selectivity in CO ₂ Catalytic Reduction. Journal of the American Chemical Society, 2018, 140, 13736-13745.	13.7	210
7	Catalyst deactivation via decomposition into single atoms and the role of metal loading. Nature Catalysis, 2019, 2, 748-755.	34.4	171
8	Uniformity Is Key in Defining Structure–Function Relationships for Atomically Dispersed Metal Catalysts: The Case of Pt/CeO ₂ . Journal of the American Chemical Society, 2020, 142, 169-184.	13.7	170
9	Uniform Catalytic Site in Sn-β-Zeolite Determined Using X-ray Absorption Fine Structure. Journal of the American Chemical Society, 2005, 127, 12924-12932.	13.7	147
10	Determining the location and nearest neighbours of aluminium in zeolites with atom probe tomography. Nature Communications, 2015, 6, 7589.	12.8	139
11	Surface phase transitions in co chemisorption on pt{110}. Surface Science, 1982, 117, 245-256.	1.9	135
12	Generation of atomic oxygen on Ag(111) and Ag(110) using NO2: a TPD, LEED, HREELS, XPS and NRA study. Surface Science, 1995, 342, 185-198.	1.9	128
13	Sensitivity of Pt x-ray absorption near edge structure to the morphology of small Pt clusters. Journal of Chemical Physics, 2002, 116, 1911-1919.	3.0	128
14	The chemisorption and decomposition of ethylene and acetylene on Ni(110). Surface Science, 1984, 148, 499-525.	1.9	126
15	Uniform Pt/Pd Bimetallic Nanocrystals Demonstrate Platinum Effect on Palladium Methane Combustion Activity and Stability. ACS Catalysis, 2017, 7, 4372-4380.	11.2	124
16	Structural Characteristics and Reactivity/Reducibility Properties of Dispersed and Bilayered V2O5/TiO2/SiO2 Catalysts. Journal of Physical Chemistry B, 1999, 103, 618-629.	2.6	117
17	Vibrational studies of the surface phases of CO on Pt{110} at 300 K. Surface Science, 1984, 144, 347-369.	1.9	113
18	Characterization of the adsorption and decomposition of methanol on Ni(110). Surface Science, 1985, 150, 399-418.	1.9	103

#	Article	IF	CITATIONS
19	In-Situ XANES of Carbon-Supported Ptâ^'Ru Anode Electrocatalyst for Reformate-Air Polymer Electrolyte Fuel Cells. Journal of Physical Chemistry B, 2002, 106, 3458-3465.	2.6	97
20	Ammonia synthesis over iron single-crystal catalysts: the effects of alumina and potassium. The Journal of Physical Chemistry, 1986, 90, 4726-4729.	2.9	92
21	Synthesis of Colloidal Pd/Au Dilute Alloy Nanocrystals and Their Potential for Selective Catalytic Oxidations. Journal of the American Chemical Society, 2018, 140, 12930-12939.	13.7	92
22	Local site symmetry of dispersed molybdenum oxide catalysts: XANES at the Mo L2,3-edges. The Journal of Physical Chemistry, 1993, 97, 6048-6053.	2.9	87
23	Effect of Hydrogen Adsorption on the X-Ray Absorption Spectra of Small Pt Clusters. Physical Review Letters, 2001, 86, 1642-1645.	7.8	86
24	Observation of Structure-Induced Surface Vibrational Resonances on Metal Surfaces. Physical Review Letters, 1985, 54, 1428-1431.	7.8	83
25	Experimental (XAS, STEM, TPR, and XPS) and Theoretical (DFT) Characterization of Supported Rhenium Catalysts. Journal of Physical Chemistry C, 2011, 115, 5740-5755.	3.1	83
26	Directing reaction pathways via in situ control of active site geometries in PdAu single-atom alloy catalysts. Nature Communications, 2021, 12, 1549.	12.8	82
27	Structure, Dynamics, and Reactivity for Light Alkane Oxidation of Fe(II) Sites Situated in the Nodes of a Metal–Organic Framework. Journal of the American Chemical Society, 2019, 141, 18142-18151.	13.7	80
28	Probing Atomic Distributions in Mono- and Bimetallic Nanoparticles by Supervised Machine Learning. Nano Letters, 2019, 19, 520-529.	9.1	80
29	Electronic properties and charge transfer phenomena in Pt nanoparticles on Î ³ -Al2O3: size, shape, support, and adsorbate effects. Physical Chemistry Chemical Physics, 2012, 14, 11766.	2.8	76
30	Coke Formation in a Zeolite Crystal During the Methanolâ€ŧoâ€Hydrocarbons Reaction as Studied with Atom Probe Tomography. Angewandte Chemie - International Edition, 2016, 55, 11173-11177.	13.8	74
31	Reaction of methanol on Si(111)-7 × 7. Surface Science, 1985, 154, 35-51.	1.9	73
32	Dynamic Reorganization and Confinement of Ti ^{IV} Active Sites Controls Olefin Epoxidation Catalysis on Two-Dimensional Zeotypes. Journal of the American Chemical Society, 2019, 141, 7090-7106.	13.7	68
33	Transition state and product diffusion control by polymer–nanocrystal hybrid catalysts. Nature Catalysis, 2019, 2, 852-863.	34.4	64
34	Angle-resolved thermal desorption of N2 from W{310} and W{110}. Vacuum, 1981, 31, 503-506.	3.5	62
35	Operando high-pressure investigation of size-controlled CuZn catalysts for the methanol synthesis reaction. Nature Communications, 2021, 12, 1435.	12.8	62
36	Atomically Dispersed Reduced Graphene Aerogel-Supported Iridium Catalyst with an Iridium Loading of 14.8 wt %. ACS Catalysis, 2019, 9, 9905-9913.	11.2	55

#	Article	IF	CITATIONS
37	Hybridization peaks in Pt–Cl XANES1Supported in part by the US DOE and by UOP LLC.1. Chemical Physics Letters, 2000, 316, 495-500.	2.6	54
38	Interplay between nanoscale reactivity and bulk performance of H-ZSM-5 catalysts during the methanol-to-hydrocarbons reaction. Journal of Catalysis, 2013, 307, 185-193.	6.2	51
39	Tuning the Selectivity of Single-Site Supported Metal Catalysts with Ionic Liquids. ACS Catalysis, 2017, 7, 6969-6972.	11.2	51
40	Beyond Radical Rebound: Methane Oxidation to Methanol Catalyzed by Iron Species in Metal–Organic Framework Nodes. Journal of the American Chemical Society, 2021, 143, 12165-12174.	13.7	51
41	Chapter 6 Characterization of Catalysts in Reactive Atmospheres by Xâ€ray Absorption Spectroscopy. Advances in Catalysis, 2009, 52, 339-465.	0.2	49
42	Engineering of Ruthenium–Iron Oxide Colloidal Heterostructures: Improved Yields in CO ₂ Hydrogenation to Hydrocarbons. Angewandte Chemie - International Edition, 2019, 58, 17451-17457.	13.8	49
43	A versatile approach for quantification of surface site fractions using reaction kinetics: The case of CO oxidation on supported Ir single atoms and nanoparticles. Journal of Catalysis, 2019, 378, 121-130.	6.2	49
44	<i>In situ</i> observation of phase changes of a silica-supported cobalt catalyst for the Fischer–Tropsch process by the development of a synchrotron-compatible <i>inÂsitu/operando</i> powder X-ray diffraction cell. Journal of Synchrotron Radiation, 2018, 25, 1673-1682.	2.4	47
45	Degradation of Multiply-Chlorinated Hydrocarbons on Cu(100). Langmuir, 1997, 13, 229-242.	3.5	46
46	Pressureâ€Dependent Effect of Hydrogen Adsorption on Structural and Electronic Properties of Pt/γâ€Al ₂ O ₃ Nanoparticles. ChemCatChem, 2014, 6, 348-352.	3.7	46
47	Structural characterization of Ni–W hydrocracking catalysts using in situ EXAFS and HRTEM. Journal of Catalysis, 2009, 263, 16-33.	6.2	45
48	The influence of orientation on the H-D exchange reactions in chemisorbed aromatics: Benzene and pyridine adsorbed on Pt{110}. Surface Science, 1987, 179, 243-253.	1.9	44
49	Design and operation of a high pressure reaction cell for in situ X-ray absorption spectroscopy. Catalysis Today, 2007, 126, 18-26.	4.4	43
50	Supported VPO Catalysts for Selective Oxidation of Butane. II. Characterization of VPO/SiO2Catalysts. Journal of Physical Chemistry B, 1997, 101, 6895-6902.	2.6	42
51	Manganese oxide catalyzed methane partial oxidation in trifluoroacetic acid: Catalysis and kinetic analysis. Catalysis Today, 2009, 140, 157-161.	4.4	42
52	Expanding Beyond the Micropore: Active-Site Engineering in Hierarchical Architectures for Beckmann Rearrangement. ACS Catalysis, 2015, 5, 6587-6593.	11.2	41
53	Understanding Structure–Property Relationships of MoO ₃ -Promoted Rh Catalysts for Syngas Conversion to Alcohols. Journal of the American Chemical Society, 2019, 141, 19655-19668.	13.7	41
54	Controlling catalytic activity and selectivity for partial hydrogenation by tuning the environment around active sites in iridium complexes bonded to supports. Chemical Science, 2019, 10, 2623-2632.	7.4	40

#	Article	IF	CITATIONS
55	Direct characterization of a catalytic surface reaction step: Benzene-deuterium exchange on Pt{110}. Surface Science, 1983, 126, 349-358.	1.9	39
56	Tunable Catalytic Performance of Palladium Nanoparticles for H ₂ O ₂ Direct Synthesis via Surface-Bound Ligands. ACS Catalysis, 2020, 10, 5202-5207.	11.2	39
57	Split-Pool Method for Synthesis of Solid-State Material Combinatorial Libraries. ACS Combinatorial Science, 2002, 4, 569-575.	3.3	36
58	Highâ€Energyâ€Resolution Xâ€ray Absorption Spectroscopy for Identification of Reactive Surface Species on Supported Singleâ€6ite Iridium Catalysts. Chemistry - A European Journal, 2017, 23, 14760-14768.	3.3	35
59	Chemistry of chloroethylenes on Cu(100): bonding and reactions. Surface Science, 1997, 380, 151-164.	1.9	34
60	Comparison of ethylene oxide and propylene oxide chemisorbed on clean and oxygen precovered Ag(110). Journal of Vacuum Science and Technology A: Vacuum, Surfaces and Films, 1992, 10, 2336-2341.	2.1	33
61	Operando Effects on the Structure and Dynamics of Pt <i>_n</i> Sn _{<i>m</i>} /î³-Al ₂ O ₃ from Ab Initio Molecular Dynamics and X-ray Absorption Spectra. Journal of Physical Chemistry C, 2013, 117, 12446-12457.	3.1	33
62	Surface analysis of zeolites: An XPS, variable kinetic energy XPS, and low energy ion scattering study. Surface Science, 2016, 648, 376-382.	1.9	33
63	On the Cobalt Carbide Formation in a Co/TiO ₂ Fischer–Tropsch Synthesis Catalyst as Studied by High-Pressure, Long-Term <i>Operando</i> X-ray Absorption and Diffraction. ACS Catalysis, 2021, 11, 2956-2967.	11.2	33
64	Characterizing industrial catalysts using in situ XAFS under identical conditions. Physical Chemistry Chemical Physics, 2010, 12, 7702.	2.8	31
65	Catalytic Performance and Near-Surface X-ray Characterization of Titanium Hydride Electrodes for the Electrochemical Nitrate Reduction Reaction. Journal of the American Chemical Society, 2022, 144, 5739-5744.	13.7	31
66	Generation and Reaction of Vinyl Groups on a Cu(100) Surface. The Journal of Physical Chemistry, 1996, 100, 12431-12439.	2.9	30
67	Palladium oxidation leads to methane combustion activity: Effects of particle size and alloying with platinum. Journal of Chemical Physics, 2019, 151, 154703.	3.0	30
68	The effects of preadsorbed oxygen on the adsorption and decomposition of methanol on Ni(110). Surface Science, 1985, 155, L281-L291.	1.9	29
69	Aberrationâ€Corrected Transmission Electron Microscopy and Inâ€Situ XAFS Structural Characterization of Pt/γâ€Al ₂ O ₃ Nanoparticles. ChemCatChem, 2015, 7, 3779-3787.	3.7	29
70	Characterization of Coke on a Pt-Re/γ-Al ₂ O ₃ Re-Forming Catalyst: Experimental and Theoretical Study. ACS Catalysis, 2017, 7, 1452-1461.	11.2	29
71	Core-shell and egg-shell zeolite catalysts for enhanced hydrocarbon processing. Journal of Catalysis, 2022, 405, 664-675.	6.2	29
72	Surface Structure of Highly Dispersed MoO3on MgO Using in Situ Mo L3-Edge XANESâ€. Langmuir, 1998, 14, 1500-1504.	3.5	28

#	Article	IF	CITATIONS
73	A Theory-Guided X-ray Absorption Spectroscopy Approach for Identifying Active Sites in Atomically Dispersed Transition-Metal Catalysts. Journal of the American Chemical Society, 2021, 143, 20144-20156.	13.7	28
74	Mechanistic and Electronic Insights into a Working NiAu Single-Atom Alloy Ethanol Dehydrogenation Catalyst. Journal of the American Chemical Society, 2021, 143, 21567-21579.	13.7	28
75	Simple flow through reaction cells for in situ transmission and fluorescence x-ray-absorption spectroscopy of heterogeneous catalysts. Review of Scientific Instruments, 2006, 77, 023105.	1.3	27
76	Fe Coordination Environment, Fe-Incorporated Ni(OH) ₂ Phase, and Metallic Core Are Key Structural Components to Active and Stable Nanoparticle Catalysts for the Oxygen Evolution Reaction. ACS Catalysis, 2022, 12, 1992-2008.	11.2	27
77	Role of Co ₂ C in ZnOâ€promoted Co Catalysts for Alcohol Synthesis from Syngas. ChemCatChem, 2019, 11, 799-809.	3.7	26
78	An in situ x-ray absorption spectroscopic cell for high temperature gas-flow measurements. Review of Scientific Instruments, 1998, 69, 2618-2621.	1.3	24
79	Transmission and fluorescence X-ray absorption spectroscopy cell/flow reactor for powder samples under vacuum or in reactive atmospheres. Review of Scientific Instruments, 2016, 87, 073108.	1.3	24
80	Insights and comparison of structure–property relationships in propane and propene catalytic combustion on Pd- and Pt-based catalysts. Journal of Catalysis, 2021, 401, 89-101.	6.2	24
81	Colloidal Platinum–Copper Nanocrystal Alloy Catalysts Surpass Platinum in Low-Temperature Propene Combustion. Journal of the American Chemical Society, 2022, 144, 1612-1621.	13.7	24
82	Spectroscopic and Computational Insights on Catalytic Synergy in Bimetallic Aluminophosphate Catalysts. Journal of the American Chemical Society, 2015, 137, 8534-8540.	13.7	23
83	Dynamic Surface Reconstruction Unifies the Electrocatalytic Oxygen Evolution Performance of Nonstoichiometric Mixed Metal Oxides. Jacs Au, 2021, 1, 2224-2241.	7.9	23
84	Tilted CO chemisorbed on Pt {110}. Vacuum, 1981, 31, 463-465.	3.5	20
85	Probing the Location and Speciation of Elements in Zeolites with Correlated Atom Probe Tomography and Scanning Transmission Xâ€Ray Microscopy. ChemCatChem, 2019, 11, 488-494.	3.7	19
86	Unraveling the individual influences of supports and ionic liquid coatings on the catalytic properties of supported iridium complexes and iridium clusters. Journal of Catalysis, 2020, 387, 186-195.	6.2	18
87	Characterization of the adsorption and decomposition of methanol on Ni(110). Surface Science Letters, 1985, 150, A51.	0.1	17
88	Oxidation of cyclopropane with coadsorbed oxygen on Pt(111). Surface Science, 1997, 374, 162-168.	1.9	17
89	Electronic Structure of Atomically Dispersed Supported Iridium Catalyst Controls Iridium Aggregation. ACS Catalysis, 2020, 10, 12354-12358.	11.2	17
90	Coke Formation in a Zeolite Crystal During the Methanolâ€ŧoâ€Hydrocarbons Reaction as Studied with Atom Probe Tomography. Angewandte Chemie, 2016, 128, 11339-11343.	2.0	16

#	Article	IF	CITATIONS
91	Revealing the structure of a catalytic combustion active-site ensemble combining uniform nanocrystal catalysts and theory insights. Proceedings of the National Academy of Sciences of the United States of America, 2020, 117, 14721-14729.	7.1	16
92	Understanding Degradation Mechanisms in SrIrO ₃ Oxygen Evolution Electrocatalysts: Chemical and Structural Microscopy at the Nanoscale. Advanced Functional Materials, 2021, 31, 2101542.	14.9	16
93	Alumina-Supported Trirhenium Clusters:  Stable High-Temperature Catalysts for Methylcyclohexane Conversion. Journal of Physical Chemistry C, 2008, 112, 3383-3391.	3.1	14
94	Spatial intensity distributions from electron impact scattering modes: W{100}(1 × 1)H. Journal of Electron Spectroscopy and Related Phenomena, 1983, 29, 265-272.	1.7	13
95	Characterization of a Fluidized Catalytic Cracking Catalyst on Ensemble and Individual Particle Level by Xâ€ray Micro†and Nanotomography, Microâ€Xâ€ray Fluorescence, and Microâ€Xâ€ray Diffraction. ChemCatChem, 2014, 6, 1427-1437.	3.7	13
96	Catalytic CO Oxidation on MgAl ₂ O ₄ -Supported Iridium Single Atoms: Ligand Configuration and Site Geometry. Journal of Physical Chemistry C, 2021, 125, 11380-11390.	3.1	13
97	Monolayer Support Control and Precise Colloidal Nanocrystals Demonstrate Metal–Support Interactions in Heterogeneous Catalysts. Advanced Materials, 2021, 33, e2104533.	21.0	13
98	Steering CO ₂ hydrogenation toward C–C coupling to hydrocarbons using porous organic polymer/metal interfaces. Proceedings of the National Academy of Sciences of the United States of America, 2022, 119, .	7.1	13
99	Oxidative desulfurization of sulfur compounds: Oxidation of thiophene and derivatives with hydrogen peroxide using Ti-Beta catalyst. Studies in Surface Science and Catalysis, 2008, , 1017-1020.	1.5	12
100	Science and Technology of Framework Metal-Containing Zeotype Catalysts. Advances in Catalysis, 2014, 57, 1-97.	0.2	12
101	Enhanced alcohol production over binary Mo/Co carbide catalysts in syngas conversion. Journal of Catalysis, 2020, 391, 446-458.	6.2	12
102	The reaction of propylene with ordered and disordered oxygen atoms adsorbed on the Ag(110) surface. Surface Science, 1997, 382, 266-274.	1.9	11
103	The desorption of propylene oxide from oxygen atom and hydroxyl covered Ag(110). Surface Science, 1998, 401, 1-11.	1.9	11
104	Directed-Sorting Method for Synthesis of Bead-Based Combinatorial Libraries of Heterogeneous Catalysts. ACS Combinatorial Science, 2006, 8, 199-212.	3.3	11
105	Controlled one-step synthesis of hierarchically structured macroscopic silica spheres. Microporous and Mesoporous Materials, 2011, 146, 18-27.	4.4	10
106	Operando IV. Catalysis Today, 2013, 205, 1-2.	4.4	10
107	Insight into restructuring of Pd-Au nanoparticles using EXAFS. Radiation Physics and Chemistry, 2020, 175, 108304.	2.8	9
108	Direct observation of the kinetics of gas–solid reactions using <i>in situ</i> kinetic and spectroscopic techniques. Reaction Chemistry and Engineering, 2018, 3, 668-675.	3.7	8

#	Article	IF	CITATIONS
109	Insights into Copper Sulfide Formation from Cu and S K edge XAS and DFT studies. Inorganic Chemistry, 2020, 59, 15276-15288.	4.0	8
110	Engineering of Ruthenium–Iron Oxide Colloidal Heterostructures: Improved Yields in CO ₂ Hydrogenation to Hydrocarbons. Angewandte Chemie, 2019, 131, 17612-17618.	2.0	7
111	Reactivity of Pd–MO ₂ encapsulated catalytic systems for CO oxidation. Catalysis Science and Technology, 2022, 12, 1476-1486.	4.1	7
112	Atomically Dispersed Platinum in Surface and Subsurface Sites on MgO Have Contrasting Catalytic Properties for CO Oxidation. Journal of Physical Chemistry Letters, 2022, 13, 3896-3903.	4.6	7
113	Impurity Control in Catalyst Design: The Role of Sodium in Promoting and Stabilizing Co and Co ₂ C for Syngas Conversion. ChemCatChem, 2021, 13, 1186-1194.	3.7	6
114	Nanoscale Chemical Imaging of Coking Mechanisms in a Zeolite ZSM-5 Crystal by Atom Probe Tomography. Microscopy and Microanalysis, 2017, 23, 674-675.	0.4	5
115	Characterization of a Metal–Organic Framework Zr ₆ O ₈ Node-Supported Atomically Dispersed Iridium Catalyst for Ethylene Hydrogenation by X-ray Absorption Near-Edge Structure and Infrared Spectroscopies. Journal of Physical Chemistry C, 2021, 125, 16995-17007.	3.1	5
116	Surface Chemistry. , 2003, , 373-421.		5
117	First-Principles Approach to Extracting Chemical Information from X-ray Absorption Near-Edge Spectra of Ga-Containing Materials. Journal of Physical Chemistry C, 2021, 125, 27901-27908.	3.1	5
118	Understanding Support Effects of ZnOâ€Promoted Co Catalysts for Syngas Conversion to Alcohols Using Atomic Layer Deposition. ChemCatChem, 2021, 13, 770-781.	3.7	4
119	CO oxidation on MgAl ₂ O ₄ supported Ir _{<i>n</i>} : activation of lattice oxygen in the subnanometer regime and emergence of nuclearity-activity volcano. Journal of Materials Chemistry A, 2022, 10, 4266-4278.	10.3	4
120	Summary Abstract: Isolation of a formate intermediate in the decomposition of methanol on Ni(110)–(2×1)O. Journal of Vacuum Science and Technology A: Vacuum, Surfaces and Films, 1985, 3, 1647-1648.	2.1	3
121	In Situ X-ray Absorption Fine Structure (XAFS) Applied to Catalyst Characterization at UOP: Examples and Perspectives. Synchrotron Radiation News, 2011, 24, 12-17.	0.8	3
122	The Consortium for Operando and Advanced Catalyst Characterization via Electronic Spectroscopy and Structure (Co-ACCESS) at Stanford Synchrotron Radiation Lightsource (SSRL). Synchrotron Radiation News, 2020, 33, 15-19.	0.8	3
123	Lanthanum induced lattice strain improves hydrogen sulfide capacities of copper oxide adsorbents. AICHE Journal, 2021, 67, e17484.	3.6	3
124	Iridium pair sites anchored to Zr6O8 nodes of the metal–organic framework UiO-66 catalyze ethylene hydrogenation. Journal of Catalysis, 2022, 411, 177-186.	6.2	3
125	Identifying higher oxygenate synthesis sites in Cu catalysts promoted and stabilized by atomic layer deposited Fe2O3. Journal of Catalysis, 2021, 404, 210-223.	6.2	2
126	Transformation of reduced graphene aerogel-supported atomically dispersed iridium into stable clusters approximated as Ir6 during ethylene hydrogenation catalysis. Journal of Catalysis, 2022, 413, 603-613.	6.2	2

#	Article	IF	CITATIONS
127	In Situ XAS of Ni-W Hydrocracking Catalysts. AIP Conference Proceedings, 2007, , .	0.4	1
128	Design and Operation of an In Situ High Pressure Reaction Cell for X-Ray Absorption Spectroscopy. AlP Conference Proceedings, 2007, , .	0.4	1
129	The effects of preadsorbed oxygen on the adsorption and decomposition of methanol on Ni(110). Surface Science Letters, 1985, 155, L281-L291.	0.1	0
130	Workshop on recent advances in the application of SR to catalysis. Synchrotron Radiation News, 1995, 8, 5-5.	0.8	0
131	Workshop on <i>in situ</i> applications of xâ€ray absorption fine structure. Synchrotron Radiation News, 1996, 9, 9-9.	0.8	0
132	Synthesis, Bonding, and Reactions of π-Bonded Allyl Groups on Cu(100); Allyl Radical Ejection. Langmuir, 1998, 14, 1943-1943.	3.5	0
133	National synchrotron light source 2001 annual users' meeting. Synchrotron Radiation News, 2001, 14, 2-6.	0.8	0
134	NSLS course on EXAFS data collection and analysis. Synchrotron Radiation News, 2002, 15, 10-10.	0.8	0
135	Recent advances in the application of synchrotron radiation to catalysis. Synchrotron Radiation News, 2002, 15, 10-11.	0.8	0
136	Meeting Reports: Catalysis Research at the APS. Synchrotron Radiation News, 2005, 18, 27-28.	0.8	0
137	Meeting Report: Synchrotron Catalysis Consortium: New Opportunities for In Situ XAFS Studies of Nanocatalysis. Synchrotron Radiation News, 2006, 19, 40-42.	0.8	0
138	High-Energy-Resolution X-ray Absorption Spectroscopy for Identification of Reactive Surface Species on Supported Single-Site Iridium Catalysts. Chemistry - A European Journal, 2017, 23, 14669-14669.	3.3	0
139	Catalysis by Single Metal Atoms: What is All the Fuss About?. Synchrotron Radiation News, 2019, 32, 22-23.	0.8	0

140 Surface Chemistry. , 1988, , 63-189.

0